Journal of Dental Research
2015, Vol. 94(1) 129–139

DOI: 10.1177/0022034514553817
jdr.sagepub.com

Enhanced M1/M2 Macrophage Ratio Promotes Orthodontic Root Resorption

D. He[1,2], X. Kou[1,2], Q. Luo[1,2], R. Yang[1,2], D. Liu[1,2], X. Wang[1,2], Y. Song[1,2], H. Cao[1,2], M. Zeng[1,2], Y. Gan[3], and Y. Zhou[1,2]

Abstract

Mechanical force–induced orthodontic root resorption is a major clinical challenge in orthodontic treatment. Macrophages play an important role in orthodontic root resorption, but the underlying mechanism remains unclear. In this study, we examined the mechanism by which the ratio of M1 to M2 macrophage polarization affects root resorption during orthodontic tooth movement. Root resorption occurred when nickel–titanium coil springs were applied on the upper first molars of rats for 3 to 14 d. Positively stained odontoclasts or osteoclasts with tartrate-resistant acid phosphatase were found in resorption areas. Meanwhile, M1-like macrophages positive for CD68 and inducible nitric oxide synthase (iNOS) persistently accumulated on the compression side of periodontal tissues. In addition, the expressions of the M1 activator interferon-γ and the M1-associated pro-inflammatory cytokine tumor necrosis factor (TNF)-α were upregulated on the compression side of periodontal tissues. When the coil springs were removed at the 14th day after orthodontic force application, root resorption was partially rescued. The number of $CD68^{+}CD163^{+}$ M2-like macrophages gradually increased on the compression side of periodontal tissues. The levels of M2 activator interleukin (IL)-4 and the M2-associated anti-inflammatory cytokine IL-10 also increased. Systemic injection of the TNF-α inhibitor etanercept or IL-4 attenuated the severity of root resorption and decreased the ratio of M1 to M2 macrophages. These data imply that the balance between M1 and M2 macrophages affects orthodontic root resorption. Root resorption was aggravated by an enhanced M1/M2 ratio but was partially rescued by a reduced M1/M2 ratio.

Keywords: phenotype, orthodontics, biomechanical phenomena, macrophage activation, bone remodeling, inflammation

Introduction

Mechanical force–induced orthodontic root resorption is a major clinical challenge in orthodontic tooth movement (OTM) (Brezniak and Wasserstein 2002). This process may lead to shortened roots and affect the long-term viability of teeth and dentition (Weltman et al. 2010). Macrophages function as progenitors of osteoclasts and odontoclasts, and they appear in the initial phase of OTM to promote bone and root resorption (Brudvik and Rygh 1993a, 1993b; Teitelbaum 2000). In addition, macrophages directly produce key inflammatory mediators, such as tumor necrosis factor (TNF)-α, to induce local inflammation (Andrade et al. 2007). The detailed role of macrophages in root resorption during OTM, however, is largely unknown.

Macrophages play a key role in inflammation, immune responses, and maintenance of tissue homeostasis (Lucas et al. 2010; Mosser and Edwards 2008; Novak and Koh 2013). They are classified into 2 distinct phenotypes in vitro, namely, classically activated M1 and alternatively activated M2; M1 macrophages are stimulated by Th1 cytokines such as interferon (IFN)-γ or lipopolysaccharide, whereas M2 macrophages are activated by Th2 cytokines, such as interleukin (IL)-4 or IL-13 (Gordon 2003; Gordon

[1]Department of Orthodontics, Peking University School and Hospital of Stomatology, Haidian District, Beijing, P.R. China
[2]Center for Craniofacial Stem Cell Research and Regeneration, Peking University School and Hospital of Stomatology, Haidian District, Beijing, P.R. China
[3]Center for Temporomandibular Disorders and Orofacial Pain, Peking University School and Hospital of Stomatology, Haidian District, Beijing, P.R. China

A supplemental appendix to this article is published electronically only at http://jdr.sagepub.com/supplemental.

Corresponding Author:
Y. Zhou, Department of Orthodontics, Peking University School and Hospital of Stomatology, 22# Zhongguancun South Avenue, Haidian District, Beijing, China 100081.
Email: yanhengzhou@gmail.com

and Taylor 2005; Mosser and Edwards 2008). In addition, M1 macrophages promote inflammation by producing large amounts of nitric oxide (NO) and pro-inflammatory cytokines, such as TNF-α (Dale et al. 2008), whereas M2 macrophages inhibit inflammation by producing IL-10 and arginase I (Wang et al. 2007; Hunter et al. 2010). Macrophages play different roles in mediating inflammation or maintaining tissue homeostasis because of their remarkable plasticity to change to M1 or M2 polarization depending on different environmental conditions (Sindrilaru et al. 2011; Novak and Koh 2013). Macrophage-mediated inflammatory root resorption can be rested and partially rescued by discontinued force application (Weltman et al. 2010). Therefore, we hypothesized that M1 and M2 polarization could be involved in orthodontic root resorption.

Mechanical force is required to induce OTM and root resorption. It can also stimulate inflammatory response in periodontal ligament cells (PDLCs) (Kook et al. 2011; Lee et al. 2012). The mechanism by which multiple cells and immune elements collectively mediate bone and root resorption, however, remains unclear. Moreover, whether mechanical force–induced inflammatory response in PDLCs activates macrophage-mediated root resorption remains unknown.

This study aims to examine the mechanism by which M1 and M2 macrophage polarization affects mechanical force–induced orthodontic root resorption.

Materials and Methods

Animals

Adult male Sprague–Dawley rats (180 to 200 g, 6 to 7 weeks old) were used in this study. The experimental protocols were approved by the Animal Use and Care Committee of Peking University (LA2013-92).

Application of Orthodontic Devices and Retention

The animals were anesthetized with pentobarbital sodium (40 mg/kg body weight). Mechanical force application was performed as previously described with modifications (Gonzales et al. 2010). A nickel–titanium coil spring (wire size, 0.2 mm; diameter, 1 mm; Smart Technology, Beijing, China) was connected between the right maxillary first molar and maxillary incisors to provide a nearly constant force of approximately 60 g at activation. The contralateral side served as a control. After 14 d, the spring was removed and the tooth movement space was maintained for another 14 d by placing a resin between the right maxillary first and second molars for retention. All rats were randomly divided into different groups according to the different time points of force application (F1, F3, F5, F7, and F14 d) and retention (R3, R7, and R14 d). Three to 5 rats were used at each time point.

Injection of the TNF-α Inhibitor Etanercept or IL-4

Additional rats were used to confirm the roles of M1- and M2-like macrophages in root resorption. The first batch of rats was randomly divided into 2 groups. The vehicle group was intraperitoneally injected with phosphate buffer saline (PBS), and the other group with the TNF-α inhibitor etanercept (250 μg/rat; Wyeth, Madison, NJ). The rats were injected every other day during force application. Another batch of rats was randomly divided into 2 groups. The vehicle group was intravenously injected with PBS, and the other group with murine IL-4 (0.8 μg/rat; 214–14, Peprotech, Rocky Hill, NJ). The rats were injected every day during force application. All rats received approximately 60 g of mechanical force for 12 days. Each group comprised 5 to 6 rats.

Histology and Tartrate-Resistant Acid Phosphatase (TRAP) Staining

Maxillae were collected, fixed in 4% paraformaldehyde, demineralized in 15% ethylenediaminetetraacetic acid, and then embedded by paraffin. Consecutive horizontal sections (4 μm) were obtained from the middle to apical third of each maxillary first molar. The sections from similar position of the roots were used for histological study. Hematoxylin–eosin (HE) staining was used for descriptive histology, whereas TRAP staining was performed to detect osteoclasts and odontoclasts using a leukocyte acid phosphatase kit (387A-1KT, Sigma-Aldrich, St. Louis, MO).

Immunohistochemistry

Immunohistochemistry was performed with a 2-step detection kit (Zhongshan Golden Bridge Biotechnology, Beijing, China) as previously described (Wu et al. 2010). Primary antibodies against rat TNF-α (1:150; ab1793, Abcam, Cambridge, UK), IL-10 (1:200; sc-365858, Santa Cruz, Dallas, TX), IFN-γ (1:50; sc-1377, Santa Cruz), and IL-4 (1:100; sc-53084, Santa Cruz) were used.

Immunofluorescence Staining

Immunofluorescence staining was performed as previously described (Kou et al. 2011). The sections were double stained with antibodies of anti-CD68 (1:600; MCA341GA, AbD Serotec, Oxford, UK) and anti-iNOS (1:100; ab-15323, Abcam) or anti-CD68 and anti-CD163 (1:100; sc-33560, Santa Cruz) to detect M1- or M2-like macrophages, respectively. Other sections were double stained with antibodies of anti-IFN-γ and anti-CD3 (1:50, ab828, Abcam), anti-IFN-γ and anti-NCR1 (1:100, bs2417R, Bioss, Woburn, MA), anti-IFN-γ and anti-vimentin (1:100, bs-8533R, Bioss), or anti-IL-4 and anti-CD3 to detect the sources of

IFN-γ or IL-4. Sections were then incubated with fluorescein isothiocyanate-conjugated or tetramethylrhodamine isothiocyanate-conjugated secondary antibody (1:200, Jackson Immuno Research Laboratories, West Grove, PA). Nuclei were counterstained with 4′,6-diamidino-2-phenylindole (DAPI). Confocal microscopic images were acquired using a laser scanning microscope (LSM 510, Zeiss, Jena, Germany), and the images were processed using LSM 5 Release 4.2 software. For semiquantification, the ratios of double-labeled positive cells and M1/M2 were calculated ($n = 5$).

Micro–Computed Tomography (CT) Scanning and Measurement of Root Resorption

The maxillae of rats were scanned with a micro-CT system (Inveon MMCT, Berlin, Germany) at 80 kV, 500 μA, and an image voxel size of 18 μm. Mimics 13.1 software (Materialise, Leuven, Belgium) was used for 3D image reconstruction and segmentation. The distal roots of each molar in which resorption mainly showed up were segmented from the furcation and used to calculate resorption volume with Geomagic studio 9 (3D Systems, Rock Hill, SC). Root resorption volume was measured on the basis of a 3D convex hull algorithm as previously described (Zhao et al. 2012). Resorption areas were smoothed manually on each slide referring to roots on the control side, which enabled the resorption volume to be calculated automatically. The investigators were blinded to the experimental design.

Human Primary Periodontal Ligament Cells (PDLCs) Culture and Static Compressive Force Application

The protocol used to obtain human tissue samples was approved by the Ethical Guidelines of Peking University (PKUSSIRB-201311103) and was performed with appropriate informed consents. Human PDLCs were isolated from periodontal ligament of normal orthodontic extracted bicuspids as previously described (Seo et al. 2004). PDLCs were used at passage 4 and cultured with alpha modification of Eagle's medium containing 15% fetal calf serum (GIBCO, Carlsbad, CA), 100 U/mL penicillin, and 100 g/mL streptomycin (Biofluids, Rockville, MD).

Static compressive force was applied on primary cultured PDLCs as previously described (Mitsui et al. 2005). Briefly, a layer of glass cover and additional metal weights on top were placed over an 80% confluent cell layer in 6-well plates. The PDLCs were subjected to continuous compressive force of different doses ranging from 0 to 2 g/cm^2 for 24 h or of 1 g/cm^2 for different times ranging from 0 to 24 h.

Quantitative Real-Time Polymerase Chain Reaction (PCR)

Total RNA was isolated from cell lysate with Trizol reagent (Invitrogen, Carlsbad, CA). Reverse transcription and real-time PCR were performed as previously described (Kou et al. 2011). The primers designed by Primer Premier 5.0 software and commercially synthesized were as follows:

Human GAPDH sense/antisense:

5′-ATGGGGAAGGTGAAGGTCG-3′/5′-GGGGTCATTGATGGCAACAATA-3′

Human IFN-γ sense/antisense:

5′-TGTCCAACGCAAAGCAATAC-3′/5′-TCGACCTCGAAACAGCATCT-3′

The efficiency of the newly designed primers was confirmed by sequencing the conventional PCR products.

Enzyme-Linked Immunosorbent Assay (ELISA)

The supernatants of cultured human PDLCs were collected after compressive force application, and the concentration of IFN-γ was quantified with the ELISA kit (R&D Systems, Minneapolis, MN) according to the manufacturer's instructions.

Statistical Analysis

Statistical analysis was performed with SPSS 13.0. All data were presented as mean ± *SD* and assessed by independent 2-tailed Student's *t* test or 1-way ANOVA. Statistical significance was considered at $P < 0.05$.

Results

Root Resorption Was Aggravated during Force Application and Partially Rescued after Force Removal

Micro-CT and TRAP staining were performed to assess the dynamic changes in root resorption. On the 3rd day of force application (F3d), root resorption slightly appeared on the compression side of the roots. On F7d, several pits and scallops appeared, indicating moderate root resorption. On F14d, severe features of root resorption, including penetrating craters and irregularly absorbed and shortened roots, were observed (Fig. 1A). Semiquantitative data showed that the resorption volume of distal roots gradually increased at the active resorption stage (Fig. 1C). At this stage, TRAP-positive odontoclasts and osteoclasts were detected on the compression side of distal roots (Fig. 1B). By contrast, the severity of root resorption gradually ameliorated from severe on the 7th day of retention (R7d) to moderate on R14d (Fig. 1A). This result indicates that root resorption was partially rescued. The resorption volume of distal roots

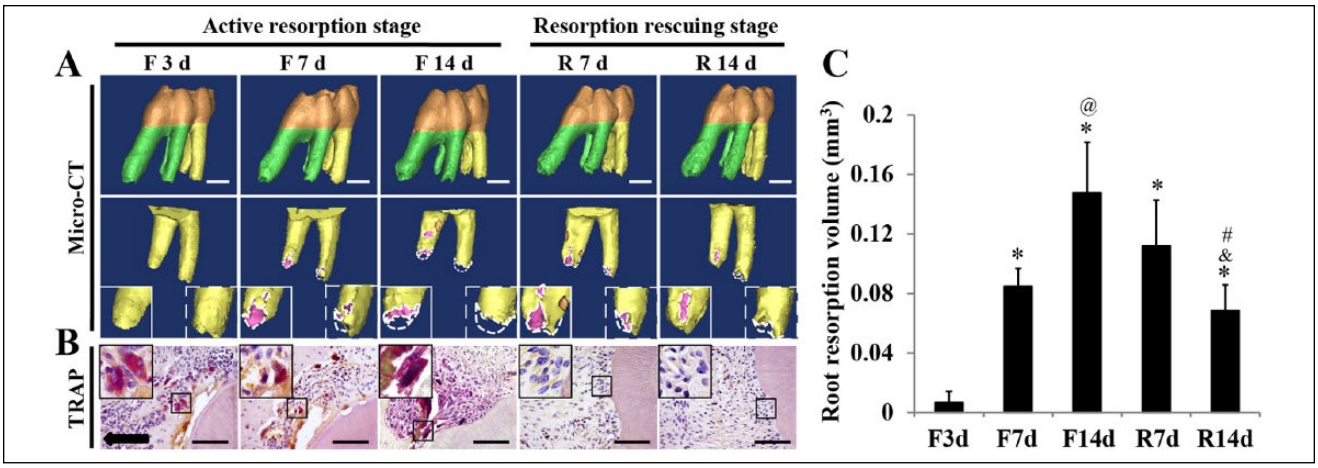

Figure 1. Dynamic changes of root resorption during force application and retention. (**A**) Micro–computed tomography (CT) images show maxillary first molars and magnified distal roots. Root resorption on the compression side of distal roots aggravated from day 3 of force application (F3d) to F7d and F14d, which gradually ameliorated in day 7 of retention (R7d) and R14d. Large boxed areas show high-magnification views of the apical third region of the distal roots. Purple areas represent the penetrating craters, and orange areas represent the shallow craters. Dashed lines outline the margins of resorption areas and the expected shape of the roots compared with the roots on the control side. Scale bars: 1000 μm. (**B**) Representative tartrate-resistant acid phosphatase (TRAP) staining images of distobuccal roots. TRAP-positive odontoclasts or osteoclasts appeared near the compression side of the roots at the active resorption stage (F3d, F7d, and F14d), but few appeared at the resorption rescuing stage (R7d and R14d). Large boxed areas show high-magnification views of the small boxed areas. Arrow represents the direction of force application. Scale bars: 100 μm. (**C**) Semiquantification of root resorption volume of distal roots by micro-CT analysis. Root resorption volume significantly increased in F7d and F14d compared with F3d, whereas it significantly decreased in R14d compared with F14d and R7d. $N = 3$ to 5; $^{*}P < 0.05$ versus F3d; $@P < 0.05$ versus F7d; $\&P < 0.05$ versus F14d; and $\#P < 0.05$ versus R7d.

was lower on R14d than it was on F14d, but it was still larger than that on F3d (Fig. 1C). TRAP-positive cells were hardly observed at this stage (Fig. 1B). These results confirm that mechanical force induces root resorption and the removal of mechanical force partially rescues root resorption in the rat model.

M1/M2 Macrophage Ratio Increased at the Active Resorption Stage and Decreased at the Resorption Rescuing Stage

Immunostaining showed that $CD68^{+}iNOS^{+}$ M1-like macrophages were remarkably infiltrated on the compression side of periodontal tissues on F3d. The infiltration of M1-like macrophages peaked on F7d and remained high until F14d. This result is consistent with the occurrence of moderate and severe root resorption from F7d to F14d at the active resorption stage. Meanwhile, $CD68^{+}CD163^{+}$ M2-like macrophages showed no alteration (Fig. 2A and 2B).

By contrast, the number of $CD68^{+}CD163^{+}$ M2-like macrophages increased on the compression side of periodontal tissues since the 3rd day of mechanical force removal and remained high until R14d. This result is consistent with the resorption rescuing stage, wherein root resorption was gradually rescued from R7d to R14d. Meanwhile, the number of M1 macrophages significantly decreased starting at the 3rd day of mechanical force removal and remained at a low level (Fig. 2A and 2B). The ratio of M1 to M2 macrophages was much more pronounced at the active resorption stage than at the resorption rescuing stage (Fig. 2C). These data indicate that alteration of the M1/M2 ratio either promotes or partially rescues root resorption.

M1 and M2 Macrophage-Associated Cytokines Contribute to Orthodontic Root Resorption

Immunohistochemistry showed that the M1-associated pro-inflammatory cytokine TNF-α was highly expressed on the compression side of periodontal tissues at the active resorption stage compared to that of the rescuing stage, which was still upregulated compared with that in the control group (Fig. 3A and 3C). Conversely, the expression level of the M2-associated anti-inflammatory cytokine IL-10 was barely detected at the active resorption stage but significantly elevated at the resorption rescuing stage (Fig. 3B and 3C).

In addition, the expression of the M1 activator IFN-γ was elevated at day 1 and remained at a high level until 14 days after force application on the compression side of periodontal tissues; however, the expression of IFN-γ disappeared at the resorption rescuing stage (Fig. 4A). The sources of IFN-γ were confirmed by double staining $IFN\text{-}\gamma^{+}CD3^{+}$ T cells and $IFN\text{-}\gamma^{+}vimentin^{+}$ PDLCs in vivo. $IFN\text{-}\gamma^{+}NCR1^{+}$ NK

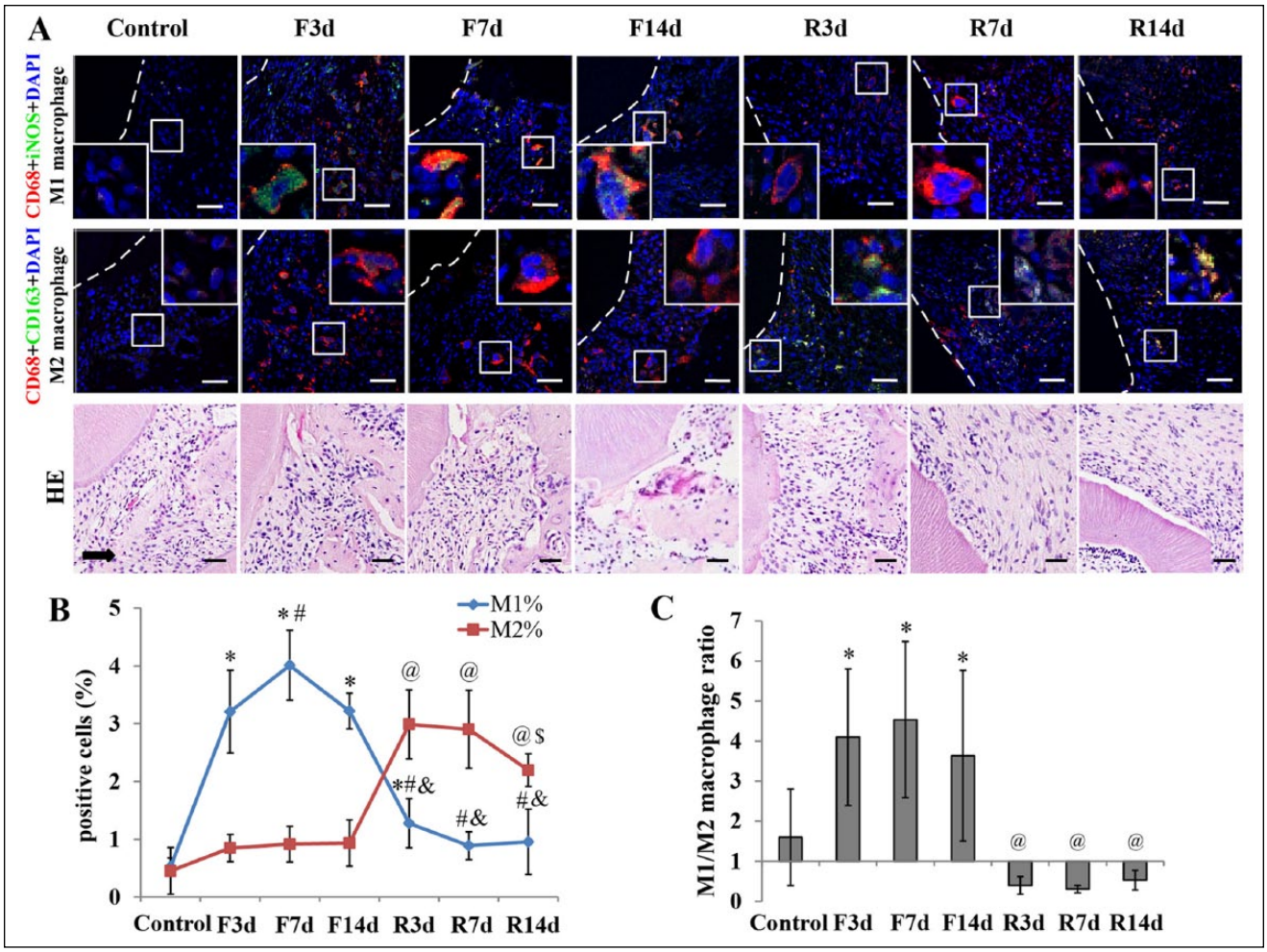

Figure 2. The M1/M2 ratio increased at the active resorption stage but decreased at the resorption rescuing stage. (**A**) Representative immunofluorescence images and hematoxylin–eosin (HE) staining on the compression side of distobuccal roots. The numbers of CD68-positive (red) and iNOS-positive (green) M1-like macrophages (merged yellow) increased at the active resorption stage (F3d, F7d, and F14d) and decreased at the resorption rescuing stage (R3d, R7d, and R14d). The numbers of CD68-positive (red) and CD163-positive (green) M2-like macrophages (merged yellow) increased at the rescuing stage. Corresponding HE staining showed the histomorphology of immunostaining sections. Arrow represents the direction of force application. Large boxed areas show high-magnification views of the small boxed areas. Dashed lines mark the outline of the roots. Scale bars: 50 μm. (**B**) Semiquantification of double-stained positive cells. The M1 proportion increased at the active resorption stage and decreased at the rescuing stage, whereas the M2 proportion increased at the rescuing stage. $N = 5$; M1-positive ratio: $^{*}P < 0.05$ versus control; $^{\#}P < 0.05$ versus F3d and F14d; $^{\&}P < 0.05$ versus F7d; M2-positive ratio: $^{@}P < 0.05$ versus control, F3d, F7d, and F14d; $^{\$}P < 0.05$ versus R3d and R7d. (**C**) Semiquantification of the M1/M2 ratio. The ratio increased at the active resorption stage and decreased at the rescuing stage. $N = 5$; $^{*}P < 0.05$ versus control; $^{@}P < 0.05$ versus F3d, F7d, and F14d.

cells were not detected (Appendix Fig. 1A–C). When static compressive force was applied to the primary cultured human PDLCs, the levels of IFN-γ mRNA expression and IFN-γ secretion in the culture supernatant were upregulated with increasing force intensity and prolonged force treatment time (Fig. 4C–F). These data suggest that both the IFN-γ secreted by T cells and the mechanical force–induced upregulated expression of IFN-γ in PDLCs provide a beneficial microenvironment to activate M1 macrophages for initiating root resorption. Conversely, the major M2 activator IL-4 was mainly detected at the resorption rescuing stage but barely detectable at the active resorption stage (Fig. 4B). The source of IL-4 was confirmed by double staining $IL\text{-}4^{+}CD3^{+}$ T cells (Appendix Fig. 1D).

TNF-α Inhibitor or IL-4 Treatment Attenuated Orthodontic Root Resorption

We systemically injected the TNF-α inhibitor etanercept to block TNF-α expression (Appendix Fig. 2). The number of

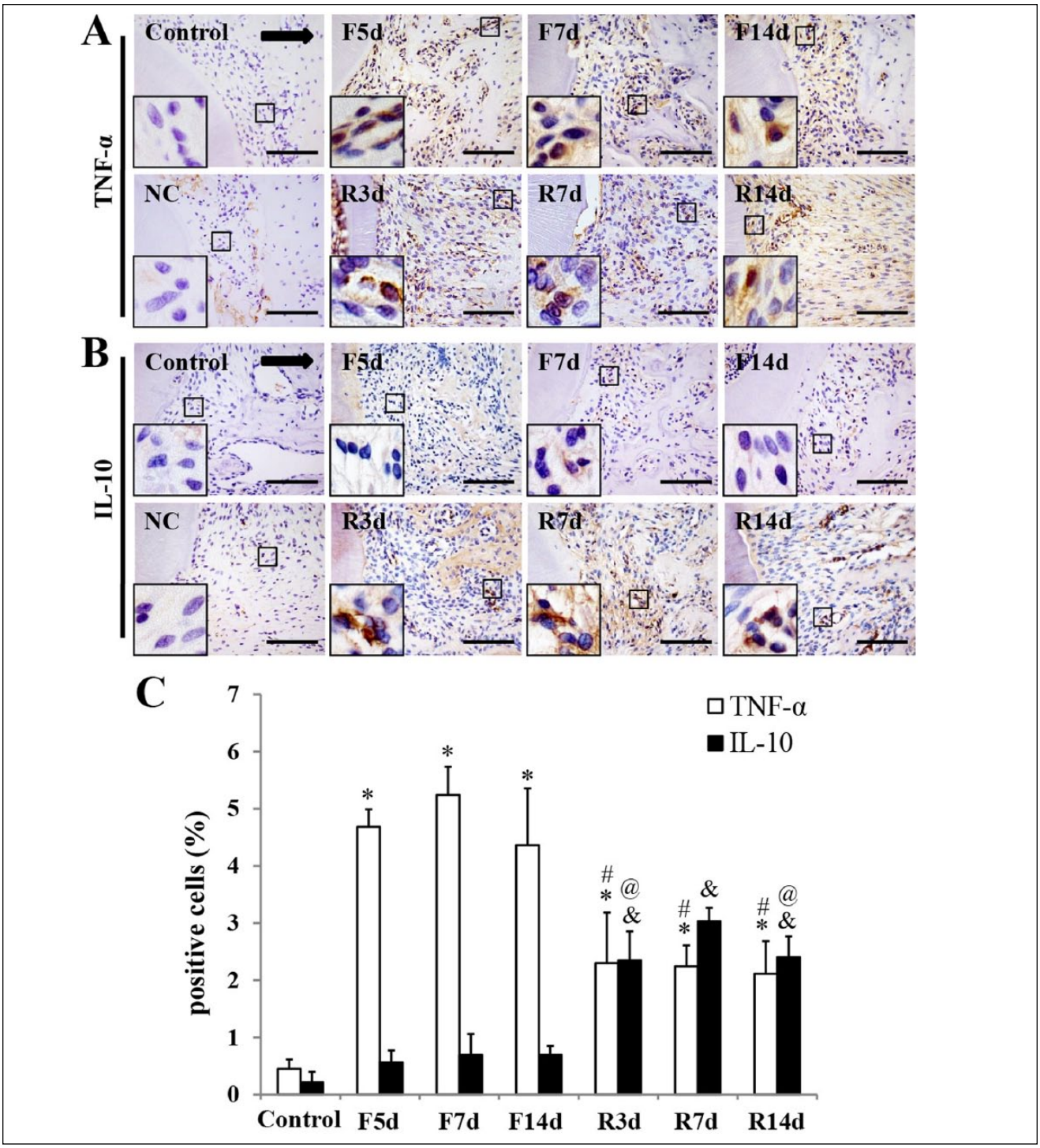

Figure 3. Different expression levels of M1 and M2 macrophage-associated cytokines at the active resorption and resorption rescuing stages. (**A, B**) Representative immunohistochemical images of the compression side of distobuccal roots. A: Tumor necrosis factor (TNF)-α staining was detected at the active resorption stage (F5d, F7d, and F14d), which decreased at the resorption rescuing stage (R3d, R7d, and R14d). B: IL-10 staining was hardly observed at the active resorption stage but appeared at the resorption rescuing stage. Large boxed areas show high-magnification views of the small boxed areas. Arrows represent the direction of force application. Scale bars: 100 μm. NC, negative control. (**C**) Semiquantification of positive cells. TNF-α expression increased at the active resorption stage (F5d, F7d, and F14d) but decreased at the rescuing stage (R3d, R7d, and R14d), although it was still upregulated compared with that in the control group. Interleukin (IL)-10 expression increased at the rescuing stage (R3d, R7d, and R14d). *N* = 5; TNF-α-positive cells: **P* < 0.05 versus control; #*P* < 0.05 versus F5d, F7d, and F14d; IL-10-positive cells: &*P* < 0.05 versus control, F5d, F7d, and F14d; @*P* < 0.05 versus R7d.

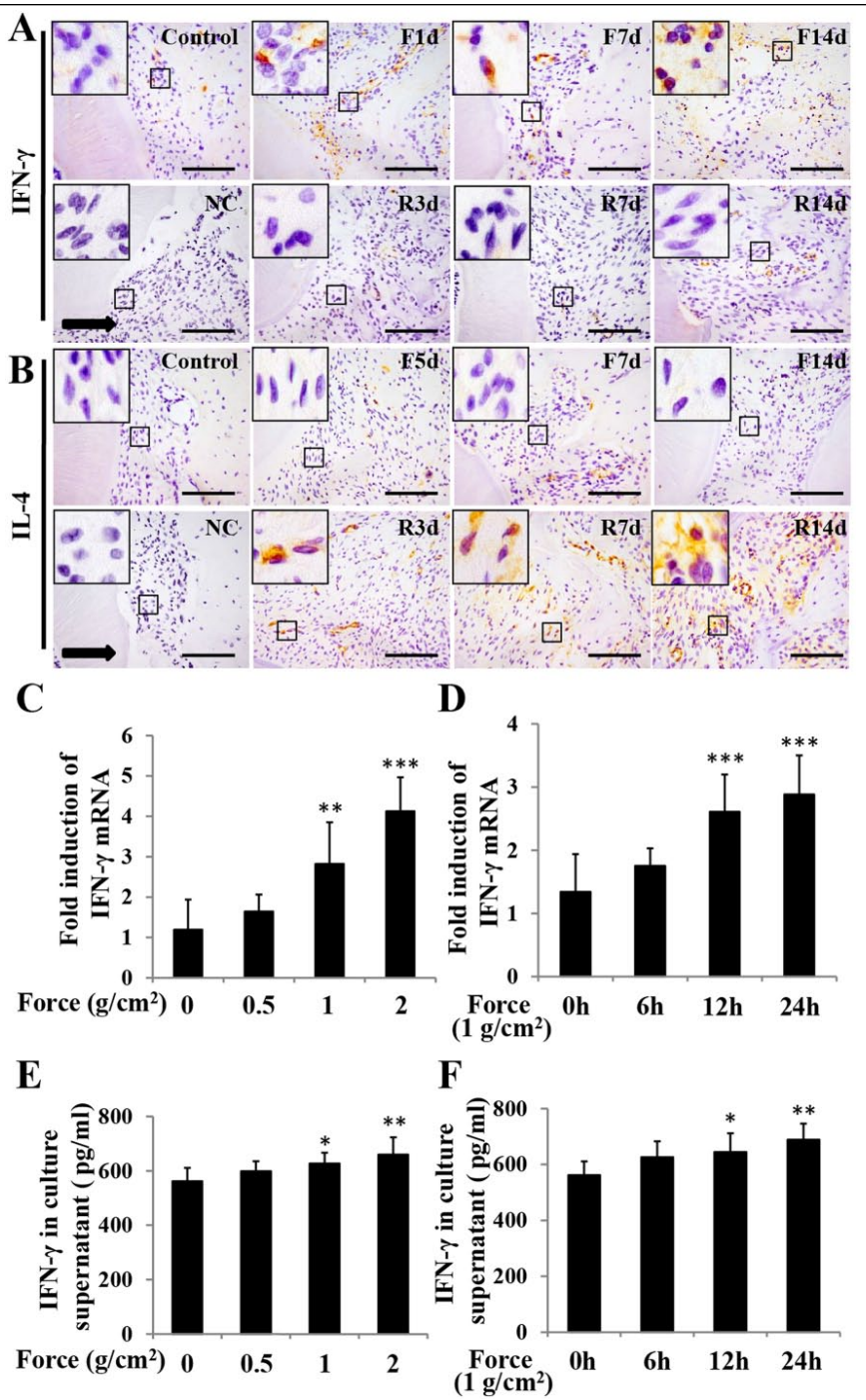

Figure 4. Mechanical force–induced upregulated expression of interferon (IFN)-γ at the active resorption stage and interleukin (IL)-4 at the resorption rescuing stage. (**A, B**) Representative immunohistochemical images of the compression side of distobuccal roots. A: IFN-γ staining was strong at the active resorption stage (F1d, F7d, and F14d) but barely detected at the resorption rescuing stage (R3d, R7d, and R14d). B: IL-4 staining appeared at the resorption rescuing stage. Large boxed areas show high-magnification views of the small boxed areas. Arrows represent the direction of force application. Scale bars: 100 μm. (**C, D**) IFN-γ mRNA expression after compressive force application in primary cultured periodontal ligament cells (PDLCs) detected by real-time polymerase chain reaction (PCR). IFN-γ mRNA expression significantly upregulated after compressive force application at 1 and 2 g/cm^2 for 24 h (N = 3; $^{**}P < 0.01$, $^{***}P < 0.001$ vs. 0 g/cm^2), as well as at 12 and 24 h time intervals after applying 1 g/cm^2 compressive force (N = 3; $^{***}P < 0.001$ vs. 0 h). (**E, F**) IFN-γ secretion after compressive force application in primary cultured PDLCs shown by enzyme-linked immunosorbent assay. IFN-γ production significantly upregulated after compressive force application at 1 and 2 g/cm^2 for 24 h (N = 3; $^{*}P < 0.05$, $^{**}P < 0.01$ vs. 0 g/cm^2), as well as at 12 and 24 h time intervals after applying 1 g/cm^2 compressive force. N = 3; $^{*}P < 0.05$, $^{**}P < 0.01$ versus 0 h.

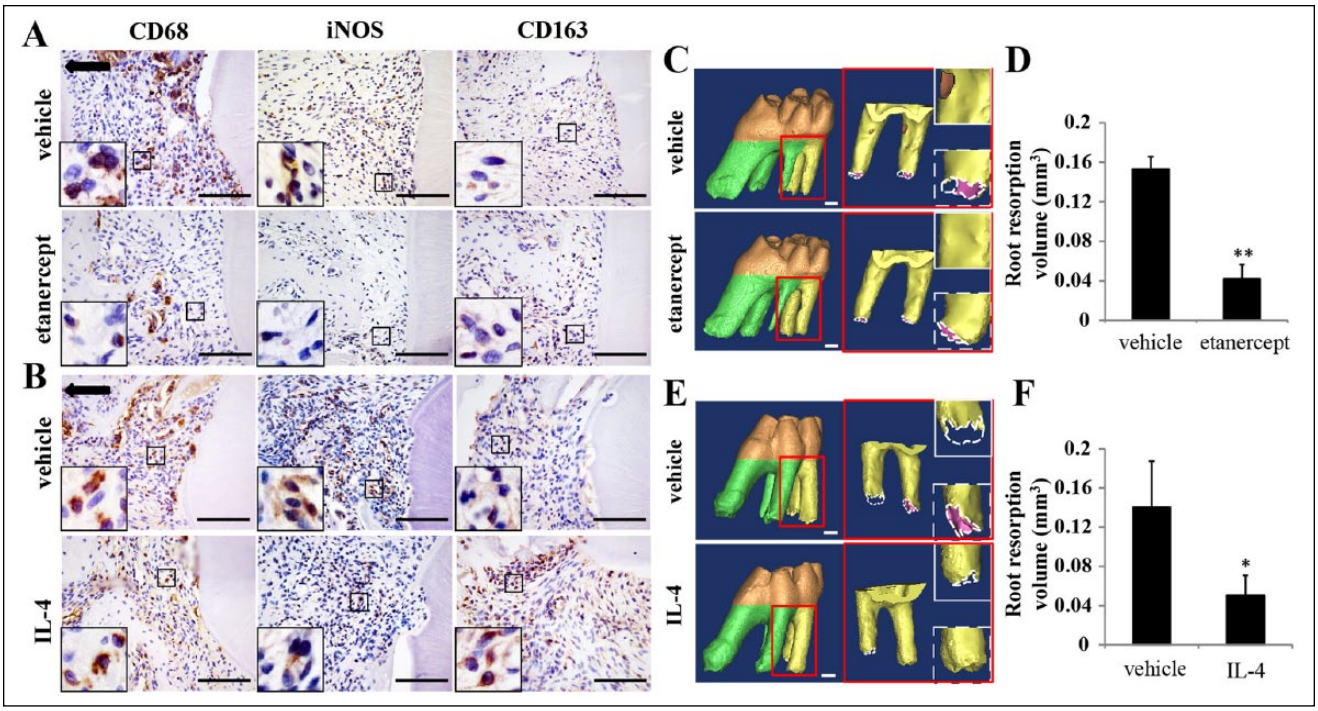

Figure 5. Injection of tumor necrosis factor (TNF)-α inhibitor or interleukin (IL)-4 decreased the M1/M2 ratio and attenuated root resorption. (**A, B**) Representative immunohistochemical images of the compression side of distobuccal roots. A: Intraperitoneal injection of the TNF-α inhibitor etanercept decreased the number of $CD68^+$ macrophages as well as the staining of iNOS on the compression side of periodontal tissues, whereas the staining of CD163 was comparable between the 2 groups. B: Changes of the number of $CD68^+$ macrophages were not detectable between the IL-4 injection group and the vehicle group. iNOS staining was downregulated, however, and CD163 staining was increased on the compression side of periodontal tissues. Large boxed areas show high-magnification views of the small boxed areas. Arrows represent the direction of force application. Scale bars: 100 μm. (**C, E**) Representative micro–computed tomography images of distal roots. Root resorption attenuated in the etanercept group and the IL-4 group compared with the vehicle group. Large boxed areas (solid and dashed) show high-magnification views of the resorption areas. Different colors mark the resorption craters and irregular root apical resorption. White dashed lines show the expected outlines of the roots compared with those on the control side. Scale bars: 500 μm. (**D, F**) Semiquantification of root resorption volume of distal roots. Root resorption volume significantly decreased in the etanercept group and the IL-4 group. $N = 5$ to 6; $^*P < 0.05$, $^{**}P < 0.01$.

$CD68^+$ macrophages on the compression side of periodontal tissues and the expression of the M1 marker iNOS decreased compared with those of the vehicle group. The expression of the M2 marker CD163 was not significantly altered, however. Consequently, the M1/M2 ratio decreased in the etanercept group (Fig. 5A). Moreover, etanercept treatment significantly attenuated distal root resorption compared to the vehicle group (Fig. 5C and 5D).

Macrophages have remarkable plasticity to respond to environmental signals. Polarized M1 can change to M2 when stimulated by IL-4 in vitro (Tacke and Zimmermann 2014). In the present study, during force application, the number of $CD68^+$ macrophages was not changed after the systemic injection of IL-4 in rats. Meanwhile, the expression of iNOS was downregulated and the expression of CD163 was upregulated on the compression side of periodontal tissues, which resulted in the reduction of the M1/M2 ratio in the IL-4 treatment group (Fig. 5B). Concomitantly, IL-4 injection significantly attenuated distal root resorption compared to the vehicle group (Fig. 5E and 5F). These data suggest that decreasing the M1/M2 ratio inhibits orthodontic root resorption.

Discussion

In this study, we provided multiple lines of evidence that the alteration of the M1/M2 macrophage ratio affects orthodontic root resorption. First, an enhanced M1/M2 ratio was detected at the active resorption stage, and a reduced M1/M2 ratio was detected at the resorption rescuing stage. Systemic injection of the TNF-α inhibitor etanercept or IL-4 decreased the ratio of M1/M2 and attenuated the severity of root resorption. Second, the M1-associated proinflammatory cytokine TNF-α and the M2-associated anti-inflammatory cytokine IL-10 were mainly detected at different stages of root resorption, playing distinctive roles

for promoting or rescuing root resorption. Third, the M1 activator IFN-γ was upregulated at the active resorption stage, whereas the M2 activator IL-4 was upregulated at the resorption rescuing stage. These data suggest that the balance between M1 and M2 macrophages contributes to orthodontic root resorption.

The changes in the ratio of M1 to M2 were associated with orthodontic root resorption. M1-like macrophages principally appeared at the active resorption stage, whereas M2-like macrophages principally appeared at the resorption rescuing stage. Previous studies have shown that M1 and M2 macrophages are involved in the early inflammatory phase or late tissue remodeling phase of wound healing (Arnold et al. 2007; Nahrendorf et al. 2007; Lucas et al. 2010). The imbalance in the M1/M2 ratio could also lead to the pathological changes in chronic inflammatory diseases, such as atherosclerosis, chronic venous leg ulcers, and osteonecrosis (Sindrilaru et al. 2011; Zhang et al. 2013). Our findings were consistent with those of the previous studies. Moreover, systemic injection of the TNF-α inhibitor etanercept or IL-4 reduced the ratio of M1 to M2 and decreased the severity of root resorption. TNF-α, as a key cytokine secreted by M1 macrophages, was considered to maintain the activation state of macrophages in an autocrine manner (Xaus et al. 2000). In addition, IL-4, as an M2 activator, can change polarized M1 to M2 in vitro (Tacke and Zimmermann 2014). Injection of the TNF-α inhibitor or IL-4 could modulate the activation state of M1 or M2, and therefore influence orthodontic root resorption. Other studies have shown that changing the M1/M2 ratio through systemic infusion of polarized M1 and M2 macrophages in mice can either increase or reduce the severity of several chronic diseases, including chronic inflammatory renal disease (Wang et al. 2007), colonic inflammation (Hunter et al. 2010), and bisphosphonate-related osteonecrosis (Zhang et al. 2013); our findings are consistent with these results. Previous studies have also reported that mechanical force changes the relative expressions of OPG and RANKL, thereby modulating osteoclast and odontoclast functions and leading to OTM and root resorption (Tyrovola et al. 2008). Macrophages, as osteoclast and odontoclast precursors, are considered important during these processes (Udagawa et al. 1990). Our study is the first to attribute mechanical force–induced orthodontic root resorption to the changes in the M1/M2 ratio, thus providing novel insights into the underlying mechanisms of orthodontic root resorption. Moreover, these findings suggest that regulating the ratio of M1 to M2 may provide a novel therapeutic strategy for the treatment of orthodontic root resorption. For example, the reduced M1/M2 ratio may inhibit the inflammation process, promote tissue repair, and thus attenuate root resorption.

The M1 and M2 macrophage-associated cytokines TNF-α and IL-10 participate in the different stages of root resorption. The distance of OTM in TNF-α receptor–deficient mice significantly decreases, indicating the importance of TNF-α signaling in alveolar bone metabolism (Andrade et al. 2007). Consistently, TNF-α was highly expressed at the active resorption stage and decreased at the rescuing stage in the present study. On the other hand, IL-10 knockout mice are susceptible to alveolar bone loss (Sasaki et al. 2004). IL-10 is also associated with the decreased severity of bone resorption in periodontitis (Sima and Glogauer 2013), indicating the rescuing role of IL-10 in alveolar bone metabolism. These previous findings support our result that IL-10 expression was upregulated at the resorption rescuing stage.

Mechanical force–induced upregulation of IFN-γ or IL-4 may activate M1 or M2 polarization at different stages of root resorption. The main IFN-γ secretor T cells were detected during the active resorption stage, whereas the NK cells were not detected. Determining whether PDLCs, as important cells in periodontal ligament, can activate M1 macrophages after mechanical force is indispensible. Previous studies have shown that PDLCs could respond to force stimuli and express multiple inflammatory elements (Lee et al. 2012). In their study, intermittent cyclic strain was used to stimulate the immortalized hPDL cell lines, which was different from our study in which static compressive force was used to stimulate the primary cultured human PDLCs. In the present study, we found that mechanical force upregulated the expression of IFN-γ in PDLCs both in vivo and in vitro, suggesting that the mechanical force–induced upregulation of IFN-γ in PDLCs may also contribute to M1 macrophage-mediated root resorption. Meanwhile, the upregulation of IL-4 secreted by T cells at the resorption rescuing stage may contribute to M2 activation.

Nevertheless, further studies with emphasis on eliminating macrophages in vivo are required to confirm the direct role of macrophages in OTM and root resorption. In addition, the heterogeneity of macrophages was shown not only by the different phenotypes of M1 and M2 in tissues but also by the different origins of heterogeneous circulating monocytes under inflammation (Hashimoto et al. 2013; Novak and Koh 2013). The roles of the different types of monocytes in OTM and root resorption warrant further investigations.

In conclusion, the balance between M1 and M2 macrophage polarization influences orthodontic root resorption. An enhanced M1:M2 ratio promotes orthodontic root resorption, whereas a reduced M1/M2 ratio partially rescues it. Alteration of the M1/M2 ratio may be a novel approach to prevent and treat orthodontic root resorption.

Author Contributions

D. He, contributed to conception, design, data acquisition, analysis, and interpretation, drafted the manuscript; X. Kou, Y. Zhou, contributed to conception, design, data analysis, and interpretation, critically revised the manuscript; Q. Luo, contributed to data analysis and interpretation, critically revised the manuscript; R. Yang, D. Liu, Y. Gan, contributed to design and data interpreta-

tion, critically revised the manuscript; X. Wang, Y. Song, contributed to design and data analysis, critically revised the manuscript; H. Cao, M. Zeng, contributed to data acquisition, critically revised the manuscript. All authors gave final approval and agree to be accountable for all aspects of the work.

Acknowledgments

This study was supported by grants from the National Natural Science Foundation of China (Grant No. 81300897) and International S&T cooperation program of China (Grant No. 2013DFB30360). The authors declare no potential conflicts of interest with respect to the authorship and/or publication of this article.

References

Andrade I Jr, Silva TA, Silva GA, Teixeira AL, Teixeira MM. 2007. The role of tumor necrosis factor receptor type 1 in orthodontic tooth movement. J Dent Res. 86(11):1089–1094.

Arnold L, Henry A, Poron F, Baba-Amer Y, van Rooijen N, Plonquet A, Gherardi RK, Chazaud B. 2007. Inflammatory monocytes recruited after skeletal muscle injury switch into antiinflammatory macrophages to support myogenesis. J Exp Med. 204(5):1057–1069.

Brezniak N, Wasserstein A. 2002. Orthodontically induced inflammatory root resorption. Part I: the basic science aspects. Angle Orthod. 72(2)175–179.

Brudvik P, Rygh P. 1993a. The initial phase of orthodontic root resorption incident to local compression of the periodontal ligament. Eur J Orthod. 15(4):249–263.

Brudvik P, Rygh P. 1993b. Non-clast cells start orthodontic root resorption in the periphery of hyalinized zones. Eur J Orthod. 15(6):467–480.

Dale DC, Boxer L, Liles WC. 2008. The phagocytes: neutrophils and monocytes. Blood. 112(4):935–945.

Gonzales C, Hotokezaka H, Darendeliler MA, Yoshida N. 2010. Repair of root resorption 2 to 16 weeks after the application of continuous forces on maxillary first molars in rats: a 2- and 3-dimensional quantitative evaluation. Am J Orthod Dentofacial Orthop. 137(4):477–485.

Gordon S. 2003. Alternative activation of macrophages. Nat Rev Immunol. 3(1):23–35.

Gordon S, Taylor PR. 2005. Monocyte and macrophage heterogeneity. Nat Rev Immunol. 5(12):953–964.

Hashimoto D, Chow A, Noizat C, Teo P, Beasley MB, Leboeuf M, Becker CD, See P, Price J, Lucas D, et al. 2013. Tissue-resident macrophages self-maintain locally throughout adult life with minimal contribution from circulating monocytes. Immunity. 38(4):792–804.

Hunter MM, Wang A, Parhar KS, Johnston MJ, Van Rooijen N, Beck PL, McKay DM. 2010. In vitro-derived alternatively activated macrophages reduce colonic inflammation in mice. Gastroenterology. 138(4):1395–1405.

Kook SH, Jang YS, Lee JC. 2011. Human periodontal ligament fibroblasts stimulate osteoclastogenesis in response to compression force through TNF-alpha-mediated activation of CD4+ T cells. J Cell Biochem. 112(10):2891–2901.

Kou XX, Wu YW, Ding Y, Hao T, Bi RY, Gan YH, Ma X. 2011. 17beta-estradiol aggravates temporomandibular joint inflammation through the NF-kappaB pathway in ovariectomized rats. Arthritis Rheum. 63(7):1888–1897.

Lee SI, Park KH, Kim SJ, Kang YG, Lee YM, Kim EC. 2012. Mechanical stress-activated immune response genes via Sirtuin 1 expression in human periodontal ligament cells. Clin Exp Immunol. 168(1):113–124.

Lucas T, Waisman A, Ranjan R, Roes J, Krieg T, Müller W, Roers A, Eming SA. 2010. Differential roles of macrophages in diverse phases of skin repair. J Immunol. 184(7):3964–3977.

Mitsui N, Suzuki N, Maeno M, Mayahara K, Yanagisawa M, Otsuka K, Shimizu N. 2005. Optimal compressive force induces bone formation via increasing bone sialoprotein and prostaglandin E(2) production appropriately. Life Sci. 77(25):3168–3182.

Mosser DM, Edwards JP. 2008. Exploring the full spectrum of macrophage activation. Nat Rev Immunol. 8(12):958–969.

Nahrendorf M, Swirski FK, Aikawa E, Stangenberg L, Wurdinger T, Figueiredo JL, Libby P, Weissleder R, Pittet MJ. 2007. The healing myocardium sequentially mobilizes two monocyte subsets with divergent and complementary functions. J Exp Med. 204(12):3037–3047.

Novak ML, Koh TJ. 2013. Phenotypic transitions of macrophages orchestrate tissue repair. Am J Pathol. 183(5):1352–1363.

Sasaki H, Okamatsu Y, Kawai T, Kent R, Taubman M, Stashenko P. 2004. The interleukin-10 knockout mouse is highly susceptible to Porphyromonas gingivalis-induced alveolar bone loss. J Periodontal Res. 39(6):432–441.

Seo BM, Miura M, Gronthos S, Bartold PM, Batouli S, Brahim J, Young M, Robey PG, Wang CY, Shi S. 2004. Investigation of multipotent postnatal stem cells from human periodontal ligament. Lancet. 364(9429):149–155.

Sima C, Glogauer M. 2013. Macrophage subsets and osteoimmunology: tuning of the immunological recognition and effector systems that maintain alveolar bone. Periodontol 2000. 63(1):80–101.

Sindrilaru A, Peters T, Wieschalka S, Baican C, Baican A, Peter H, Hainzl A, Schatz S, Qi Y, Schlecht A, et al. 2011. An unrestrained proinflammatory M1 macrophage population induced by iron impairs wound healing in humans and mice. J Clin Invest. 121(3):985–997.

Tacke F, Zimmermann HW. 2014. Macrophage heterogeneity in liver injury and fibrosis. J Hepatol. 60(5):1090–1096.

Teitelbaum SL. 2000. Bone resorption by osteoclasts. Science. 289(5484):1504–1508.

Tyrovola JB, Spyropoulos MN, Makou M, Perrea D. 2008. Root resorption and the OPG/RANKL/RANK system: a mini review. J Oral Sci. 50(4):367–376.

Udagawa N, Takahashi N, Akatsu T, Tanaka H, Sasaki T, Nishihara T, Koga T, Martin TJ, Suda T. 1990. Origin of osteoclasts: mature monocytes and macrophages are capable of differentiating into osteoclasts under a suitable microenvironment prepared by bone marrow-derived stromal cells. Proc Natl Acad Sci USA. 87(18):7260–7264.

Wang Y, Wang YP, Zheng G, Lee VW, Ouyang L, Chang DH, Mahajan D, Coombs J, Wang YM, Alexander SI, et al. 2007.

Ex vivo programmed macrophages ameliorate experimental chronic inflammatory renal disease. Kidney Int. 72(3):290–299.

Weltman B, Vig KW, Fields HW, Shanker S, Kaizar EE. 2010. Root resorption associated with orthodontic tooth movement: a systematic review. Am J Orthod Dentofacial Orthop. 137(4):462–476; discussion 412A.

Wu YW, Bi YP, Kou XX, Xu W, Ma LQ, Wang KW, Gan YH, Ma XC. 2010. 17-Beta-estradiol enhanced allodynia of inflammatory temporomandibular joint through upregulation of hippocampal TRPV1 in ovariectomized rats. J Neurosci. 30(26):8710–8719.

Xaus J, Comalada M, Valledor AF, Lloberas J, López-Soriano F, Argilés JM, Bogdan C, Celada A. 2000. LPS induces apoptosis in macrophages mostly through the autocrine production of TNF-alpha. Blood. 95(12):3823–3831.

Zhang Q, Atsuta I, Liu S, Chen C, Shi S, Shi S, Le AD. 2013. IL-17-mediated M1:M2 macrophage alteration contributes to pathogenesis of bisphosphonate-related osteonecrosis of the jaws. Clin Cancer Res. 19(12):3176–3188.

Zhao N, Liu Y, Kanzaki H, Liang W, Ni J, Lin J. 2012. Effects of local osteoprotegerin gene transfection on orthodontic root resorption during retention: an in vivo micro-CT analysis. Orthod Craniofac Res. 15(1):10–20.